

Odd-Parity Pairing and Topological Superconductivity in a Strongly Spin-Orbit Coupled Semiconductor

Satoshi Sasaki,¹ Zhi Ren,¹ A. A. Taskin,¹ Kouji Segawa,¹ Liang Fu,^{2,*} and Yoichi Ando^{1,†}

¹*Institute of Scientific and Industrial Research, Osaka University, Ibaraki, Osaka 567-0047, Japan*

²*Department of Physics, Massachusetts Institute of Technology, Cambridge, MA 02139, USA*

(Dated: March 17, 2019)

The existence of topological superconductors preserving time-reversal symmetry was recently predicted, and they are expected to provide a solid-state realization of itinerant massless Majorana fermions and a route to topological quantum computation. Their first concrete example, $\text{Cu}_x\text{Bi}_2\text{Se}_3$, was discovered last year, but the search for new materials has so far been hindered by the lack of guiding principle. Here, we report point-contact spectroscopy experiments showing that the low-carrier-density superconductor $\text{Sn}_{1-x}\text{In}_x\text{Te}$ is accompanied with surface Andreev bound states which, with the help of theoretical analysis, give evidence for odd-parity pairing and topological superconductivity. The present and previous finding of topological superconductivity in $\text{Sn}_{1-x}\text{In}_x\text{Te}$ and $\text{Cu}_x\text{Bi}_2\text{Se}_3$ demonstrates that odd-parity pairing favored by strong spin-orbit-coupling is a common underlying mechanism for materializing topological superconductivity.

PACS numbers: 74.45.+c, 74.20.Rp, 73.20.At, 03.65.Vf

Topological superconductors (TSCs) have become a research frontier in the study of topologically ordered electronic states of matter [1–4]. As a superconducting (SC) cousin of topological insulators [5, 6], a TSC supports gapless surface quasiparticle states consisting of massless Majorana fermions [3] as the hallmark of its topological order [7]. Majorana fermions are peculiar in that particles are their own antiparticles [8], and they are currently attracting significant interest because of their potential for fault-tolerant topological quantum computing [9]. The p -wave superconductor Sr_2RuO_4 has been widely discussed [10] to be an example of a chiral TSC associated with spontaneous time-reversal symmetry breaking [11]. More recently, time-reversal-invariant TSCs were theorized and attracted much attention [6]. Lately $\text{Cu}_x\text{Bi}_2\text{Se}_3$ superconductor [12] has been theoretically proposed [4] and experimentally identified [13] as the first material realization of such a TSC. However, $\text{Cu}_x\text{Bi}_2\text{Se}_3$ crystals are intrinsically inhomogeneous [14] and it has been difficult to elucidate the nature of the surface Majorana fermions. Naturally, discoveries of new TSC materials are strongly called for. In this context, $\text{Cu}_x\text{Bi}_2\text{Se}_3$ is peculiar in that it is a superconductor obtained by doping a topological insulator, and such materials are few and far between; consequently, the prospect of finding new TSC materials in doped topological insulators is not very bright.

Nevertheless, the discovery of topological superconductivity in $\text{Cu}_x\text{Bi}_2\text{Se}_3$ suggested that other TSCs might also be found in low-carrier-density semiconductors whose Fermi surface is centered around time-reversal-invariant momenta [15, 16]. This motivated us to look for signatures of topological superconductivity in In-doped SnTe (denoted $\text{Sn}_{1-x}\text{In}_x\text{Te}$) [17, 18] whose Fermi surface depicted in Fig. 1(a) satisfies the above criteria. In this Letter, by performing point-contact spectroscopy on

$\text{Sn}_{1-x}\text{In}_x\text{Te}$ single crystals, we elucidate the existence of a surface Andreev bound state (ABS) which is a hallmark of an unconventional superconductivity [19]. Knowing that the symmetry and low-energy physics of this material [20] allows only four types of superconducting gap functions and that all possible unconventional states are odd-parity [4], it is possible to conclude that $\text{Sn}_{1-x}\text{In}_x\text{Te}$ is a TSC. This discovery not only enriches the family of TSC materials for their detailed investigations, but also points to a common mechanism for topological superconductivity, providing a guiding principle for the search of TSCs.

It is known that In in $\text{Sn}_{1-x}\text{In}_x\text{Te}$ acts as an acceptor and suppresses the ferroelectric structural phase transition (SPT) in SnTe. Above $x \simeq 0.04$ the SPT is completely suppressed and the system becomes a robust superconductor whose T_c gradually increases with x up to ~ 2 K at $x \simeq 0.10$ [18]. Specific-heat measurements have confirmed bulk superconductivity with possibly a strong pairing interaction for $x = 0.044$ (where $T_c = 1.0$ K) [18], but no experiment to detect the surface ABS has been carried out so far. In this Letter, we focus on samples with $x = 0.045$ to avoid complications associated with the SPT.

$\text{Sn}_{1-x}\text{In}_x\text{Te}$ single crystals were grown by a vapor transport method. High-purity elements of Sn (99.99%), Te (99.999%), and In (99.99%) were used as starting materials. The In concentration was measured with inductively-coupled plasma atomic emission spectroscopy (ICP-AES) and was confirmed to be consistent with the observed T_c [18]. The crystallographic orientation of the surface plane was confirmed by the x-ray Laue analysis to be (001). The resistivity and the Hall resistivity were measured in the Hall-bar geometry with a six-probe method on the same crystal [Fig. 1(e)]. The Quantum Design PPMS was used as a platform to cool the sam-

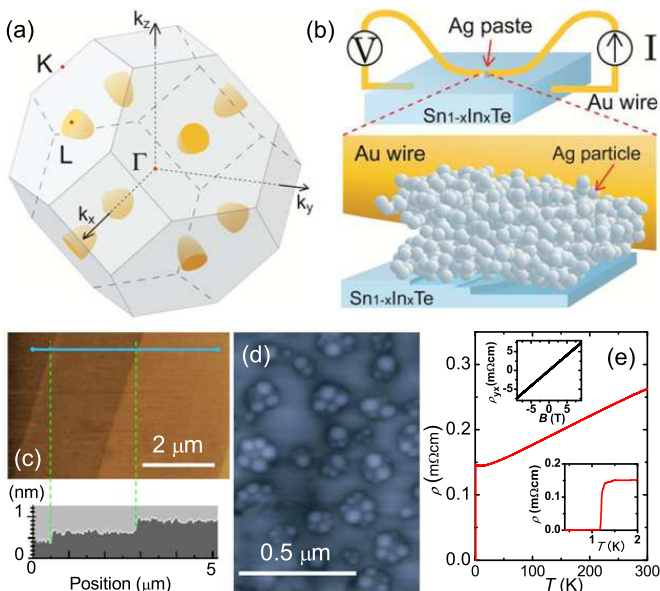


FIG. 1: (Color online) SnTe and the soft point-contact spectroscopy. (a) The Fermi surfaces of p -type SnTe are centered around the four equivalent L points, which belong to the time-reversal-invariant momenta, in the bulk Brillouin zone of the cubic NaCl structure. (b) Schematic picture of the soft point-contact spectroscopy experiment. (c) Atomic-force-microscope (AFM) picture of an as-grown faceted surface of $\text{Sn}_{1-x}\text{In}_x\text{Te}$ single crystal and its height profile. (d) AFM picture of the Ag particles on the measured surface after the gold wire is removed. (e) Temperature dependence of the resistivity of the measured sample ($x = 0.045$), showing no sign of structural phase transition. Lower inset shows a magnified view near the SC transition at 1.2 K. Upper inset shows the magnetic-field dependence of the Hall resistivity ρ_{yx} showing completely B -linear behavior, which indicates that the second valence band maxima, even if slightly populated, plays little role in our sample; the slope gives the carrier density of $8 \times 10^{20} \text{ cm}^{-3}$.

ples down to 0.37 K and apply magnetic fields up to 9 T. The upper critical field H_{c2} defined by a sharp resistivity onset was 0.3 T at 0.37 K [Fig. 2(e)].

We performed conductance spectroscopy on the faceted (001) as-grown surface [Fig. 1(c)] of $\text{Sn}_{1-x}\text{In}_x\text{Te}$ single crystals with $x = 0.045$ [$T_c = 1.2$ K, see Fig. 1(e)] using a soft point-contact technique [21] [Fig. 1(b)] which was successfully applied to $\text{Cu}_x\text{Bi}_2\text{Se}_3$ [13] to reveal its TSC nature. The soft point contacts were prepared by putting a tiny drop of silver paste below a 30- μm -diameter gold wire [Fig. 1(b)]; an atomic force microscope image of the silver nanoparticles on a measured surface is shown in Fig. 1(d). The dI/dV spectra were measured with a lock-in technique by sweeping a dc current that is superimposed with a small-amplitude [1.35 μA (rms), corresponding to 0.5 A/cm²] ac current, and a quasi-four-probe configuration was employed to read the voltage between a normal metal (silver paste) and the sample (see Ref. [13] for details). We show in the

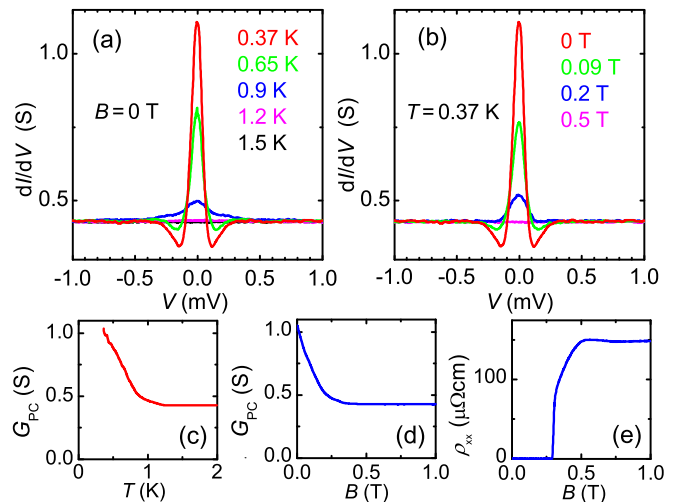


FIG. 2: (Color online) Conductance spectra of $\text{Sn}_{1-x}\text{In}_x\text{Te}$. (a) Bias-voltage (V) dependence of the differential conductance, $\frac{dI}{dV}(V)$, at various temperatures in 0 T. (b) $\frac{dI}{dV}(V)$ in various magnetic field at 0.37 K. (c) Temperature dependence of the zero-bias conductance in 0 T, showing its enhancement of more than a factor of two in the SC state at low temperature. (d) Magnetic-field (B) dependence of the zero-bias conductance at 0.37 K. (e) B dependence of the resistivity ρ_{xx} at 0.37 K showing that 0.5 T is enough to completely suppress superconductivity.

Supplemental Material [22] that this technique yields ordinary Andreev reflection spectra when applied to the conventional s -wave superconductor Sn.

When applied to $\text{Sn}_{1-x}\text{In}_x\text{Te}$, this technique allowed us to observe a signature of ABS [23] [Figs. 2(a)-2(b)], rather than the ordinary Andreev reflection; namely, the bias-voltage dependence of the differential conductance dI/dV presents a pronounced peak at zero voltage (i.e. Fermi level) accompanied by dips on its sides at the energy scale of the SC gap (± 0.1 meV). In the case of the ordinary Andreev reflection [24], as one can see in Fig. S1 of the Supplemental Material [22], two peaks, rather than dips, should be observed at the SC gap energy at low enough temperatures. Moreover, in our data for $\text{Sn}_{1-x}\text{In}_x\text{Te}$, the point-contact conductance at zero energy, G_{PC} , in the SC state becomes more than twice the normal-state value [Figs. 2(c)-2(d)], which is impossible for Andreev reflections [24] and points to the existence of ABS on the surface [19, 23].

The large magnitude of the observed zero-bias conductance peak (ZBCP) is already a strong indication that it is due to an ABS, but it is prudent to examine possible relevance of other origins of the ZBCP, such as heating effect [25], reflectionless tunneling [26], and magnetic Kondo scattering [27]. In this respect, the magnetic-field dependence of the spectra [Fig. 2(b)] gives evidence against those other possibilities (see Supplemental Material [22] for details) and one can conclude with confidence

that the observed ZBCP is caused by an inherent surface ABS. This gives strong evidence for an unconventional SC state in $\text{Sn}_{1-x}\text{In}_x\text{Te}$.

To identify the nature of the SC state in $\text{Sn}_{1-x}\text{In}_x\text{Te}$, we first note that the Fermi surface in the normal state consists of four ellipsoids centered at four L points of the face-centered-cubic (FCC) Brillouin zone. The conduction and valence bands in the vicinity of each L point are described by the $k \cdot p$ Hamiltonian [20]:

$$H(\mathbf{k}) = m\sigma_z + v\sigma_x(k_1s_2 - k_2s_1) + v_3k_3\sigma_y. \quad (1)$$

Here k_3 is the momentum along the three-fold axis ΓL ; k_2 is along the two-fold axis LK . s_i and σ_i are Pauli matrices associated with spin and orbital degrees of freedom, respectively. Specifically, the two orbitals labeled by $\sigma_z = \pm 1$ are mainly derived from the p -orbitals of Sn and Te atoms, respectively. We emphasize that at L points, these two types of p -orbitals have opposite parity and do not mix. The four-band Hamiltonian (1) of $\text{Sn}_{1-x}\text{In}_x\text{Te}$ at L points of FCC lattice is essentially equivalent to that of $\text{Cu}_x\text{Bi}_2\text{Se}_3$ at the Γ point of rhombohedral lattice [15], both of which is dictated by the underlying D_{3d} point group symmetry.

Because L points are invariant under the inversion of crystal momentum $\mathbf{k} \rightarrow -\mathbf{k}$, superconducting order parameters of zero total momentum pairing consist of four components Δ^a ($a = 1, \dots, 4$) on each Fermi pocket, and those Δ^a can be classified into the representations of the D_{3d} group at a given L point [4]. Depending on the internal spin and orbital pairing structure, there are four types of momentum-independent superconducting gap functions in A_{1g} , A_{1u} , A_{2u} and E_u representation [4]. Among these, the first one is even-parity and all the others are odd-parity.

We now discuss the pairing mechanism for $\text{Sn}_{1-x}\text{In}_x\text{Te}$ and identify the most likely pairing symmetries. First, we note that SnTe has a soft transverse optical (TO) phonon at $\mathbf{q} = \mathbf{0}$, which couples strongly to *interband* electronic excitations [28]. This phonon mode corresponds to the displacement of Sn and Te sublattice relative to each other. It becomes unstable and leads to the SPT at low temperature. The SPT temperature is suppressed by In doping [18]. As one can see in Fig. 1(e), the temperature dependence of the resistivity shows no kink down to T_c , which indicates that the SPT is completely suppressed in our sample; according to the phase diagram [18], this is reasonable for $x = 0.045$. This suggests that the TO phonon remains stable. Moreover, proximity to the SPT suggests that the tendency toward ferroelectricity is strong, which naturally points to an attractive interaction between Sn and Te p orbitals.

Given that the pairing interaction we have deduced from electron-phonon coupling is dominantly between Sn and Te, we can now establish the pairing symmetry of $\text{Sn}_{1-x}\text{In}_x\text{Te}$ following the same analysis as was done for $\text{Cu}_x\text{Bi}_2\text{Se}_3$ [4]. Essentially, the spin-orbit-coupled band

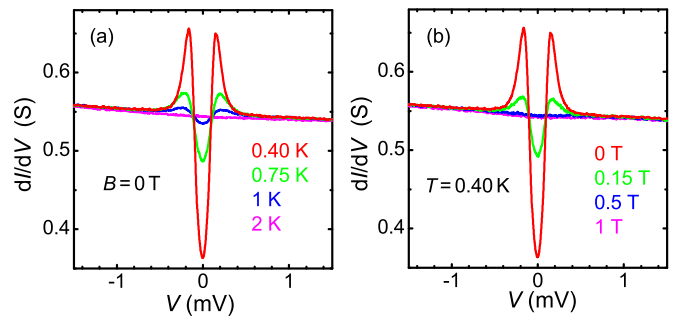


FIG. 3: (Color online) Conductance spectra of $\text{Pb}_{1-x}\text{Tl}_x\text{Te}$. (a) Bias-voltage (V) dependence of the differential conductance, $\frac{dI}{dV}(V)$, at various temperatures in 0 T. (b) $\frac{dI}{dV}(V)$ in various magnetic fields at 0.40 K. The sample ($x = 0.013$) measured here had the zero-resistivity T_c of 1.35 K and the carrier density of $1.3 \times 10^{20} \text{ cm}^{-3}$.

structure (1) cooperates with the above attractive interaction to favor the pairing between Sn and Te orbitals. Because the two orbitals have opposite parity as shown earlier, one may conclude that the pairing symmetry in $\text{Sn}_{1-x}\text{In}_x\text{Te}$ is most likely odd-parity. A detailed theory of the pairing mechanism and a full determination of the type of odd-parity pairing is beyond the scope of this paper and will be presented elsewhere. In any case, since the even-parity pairing state will not produce a surface ABS and all possible unconventional states are odd-parity in $\text{Sn}_{1-x}\text{In}_x\text{Te}$, our experimental observation indicates that the odd-parity pairing is realized in this material, which agrees with the above theoretical consideration.

On the theoretical side, odd-parity pairing has proven to host topological superconductivity under general circumstances [4, 29], similar to the way odd-parity band structure leads to topological insulators [30]. In general, a time-reversal-invariant odd-parity TSC state manifests itself in the gapless surface ABS hosting two-dimensional Majorana fermions. Therefore, one can naturally expect that this ABS gives rise to the observed spectra in point-contact measurements. In fact, given the similarity in both band structure and pairing symmetry between $\text{Cu}_x\text{Bi}_2\text{Se}_3$ and $\text{Sn}_{1-x}\text{In}_x\text{Te}$, the calculations of the surface ABS performed for $\text{Cu}_x\text{Bi}_2\text{Se}_3$ [13, 15, 31, 32] should also hold qualitatively for $\text{Sn}_{1-x}\text{In}_x\text{Te}$. This means that the observed ZBCP is exactly what is theoretically expected for this type of TSC.

Finally, we have also studied a similar superconducting material $\text{Pb}_{1-x}\text{Tl}_x\text{Te}$ with the same point-contact technique [33]. Both $\text{Sn}_{1-x}\text{In}_x\text{Te}$ and $\text{Pb}_{1-x}\text{Tl}_x\text{Te}$ superconduct at 1 – 2 K [34], crystallize in NaCl structure, and have similar band structures. Nevertheless, we found no evidence for a TSC state in $\text{Pb}_{1-x}\text{Tl}_x\text{Te}$ (Fig. 3); the observed data is consistent with the Andreev reflection spectra of conventional SC state with a low contact transparency (close to the tunneling limit). The occurrence of

the conventional SC state here is probably because the pairing interaction in $\text{Pb}_{1-x}\text{Tl}_x\text{Te}$ is dominated by the charge Kondo mechanism [34] which leads to ordinary s -wave pairing. This comparison seems to indicate the importance of the TO phonon for TSC in this class of materials.

The discovery of topological superconductivity in $\text{Sn}_{1-x}\text{In}_x\text{Te}$ reported here is instructive for further explorations of new TSCs: It gives us a guiding principle to look for semiconductors with strong spin-orbit coupling and having Fermi surfaces surrounding time-reversal-invariant momenta, because the occurrence of TSC in both $\text{Cu}_x\text{Bi}_2\text{Se}_3$ and $\text{Sn}_{1-x}\text{In}_x\text{Te}$ strongly suggests a common mechanism. In addition, this discovery has a practical importance: While the previously discovered TSC material $\text{Cu}_x\text{Bi}_2\text{Se}_3$ suffers a problem of intrinsic inhomogeneity [14] which hindered detailed studies, high-quality single crystals of $\text{Sn}_{1-x}\text{In}_x\text{Te}$ with 100% SC volume fraction are readily available. Hence, $\text{Sn}_{1-x}\text{In}_x\text{Te}$ makes it possible to explore the new topological state of matter, the time-reversal-invariant TSC, on a robust platform for the first time.

We thank T. Ueyama and R. Yoshida for technical assistance. This work was supported by JSPS (NEXT Program), MEXT (Innovative Area “Topological Quantum Phenomena” KAKENHI), and AFOSR (AOARD 124038).

* Electronic address: liangfu@mit.edu

† Electronic address: y'ando@sanken.osaka-u.ac.jp

- [1] A. P. Schnyder, S. Ryu, A. Furusaki, and A. W. W. Ludwig, *Phys. Rev. B* **78**, 195125 (2008).
- [2] M. M. Salomaa and G. E. Volovik, *Phys. Rev. B* **37**, 9298 (1988).
- [3] X.-L. Qi, T. L. Hughes, S. Raghu, and S.-C. Zhang, *Phys. Rev. Lett.* **102**, 187001 (2009).
- [4] L. Fu and E. Berg, *Phys. Rev. Lett.* **105**, 097001 (2010).
- [5] M. Z. Hasan and C. L. Kane, *Rev. Mod. Phys.* **82**, 3045 (2010).
- [6] X.-L. Qi and S.-C. Zhang, *Rev. Mod. Phys.* **83**, 1057 (2011).
- [7] X. G. Wen, *Int. J. Mod. Phys. B* **4**, 239 (1990).
- [8] F. Wilczek, *Nature Phys.* **5**, 614 (2009).
- [9] J. Alicea, *Rep. Prog. Phys.* **75**, 076501 (2012); C. W. J. Beenakker, arXiv:1112.1950.
- [10] Y. Maeno, S. Kittaka, T. Nomura, S. Yonezawa, and K. Ishida, *J. Phys. Soc. Jpn.* **81**, 011009 (2012).
- [11] N. Read and D. Green, *Phys. Rev. B* **61**, 10267 (2000).
- [12] Y. S. Hor, A. J. Williams, J. G. Checkelsky, P. Roushan, J. Seo, Q. Xu, H. W. Zandbergen, A. Yazdani, N. P. Ong, and R. J. Cava, *Phys. Rev. Lett.* **104**, 057001 (2010).
- [13] S. Sasaki, M. Kriener, K. Segawa, K. Yada, Y. Tanaka, M. Sato, and Y. Ando, *Phys. Rev. Lett.* **107**, 217001 (2011).
- [14] M. Kriener, K. Segawa, Z. Ren, S. Sasaki, S. Wada, S. Kuwabata, and Y. Ando, *Phys. Rev. B* **84**, 054513 (2011).
- [15] T. H. Hsieh and L. Fu, *Phys. Rev. Lett.* **108**, 107005 (2012).
- [16] K. Michaeli and L. Fu, arXiv:1203.1055.
- [17] G. S. Bushmarina, I. A. Drabkin, V. V. Kompaniets, R. V. Parfen'ev, D. V. Shamshur, and M. A. Shakhov, *Sov. Phys. Solid State* **28**, 612 (1986).
- [18] A. S. Erickson, J.-H. Chu, M. F. Toney, T. H. Geballe, and I. R. Fisher, *Phys. Rev. B* **79**, 024520 (2009).
- [19] S. Kashiwaya and Y. Tanaka, *Rep. Prog. Phys.* **63**, 1641 (2000).
- [20] T. H. Hsieh, H. Lin, J. Liu, W. Duan, A. Bansil, and L. Fu, arXiv:1202.1003 (to be published in *Nature Commun.*).
- [21] D. Daghero and R. S. Gonnelli, *Supercond. Sci. Technol.* **23**, 043001 (2010).
- [22] See Supplemental Material at [URL will be inserted by publisher] for supplemental data, and discussions.
- [23] Y. Tanaka and S. Kashiwaya, *Phys. Rev. Lett.* **74**, 3451 (1995).
- [24] G. E. Blonder, M. Tinkham, and T. M. Klapwijk, *Phys. Rev. B* **25**, 4515 (1982).
- [25] G. Sheet, S. Mukhopadhyay, and P. Raychaudhuri, *Phys. Rev. B* **69**, 134507 (2004).
- [26] C. W. J. Beenakker, *Phys. Rev. B* **46**, 12841(R) (1992).
- [27] L. Y. L. Shen and J. M. Rowell, *Phys. Rev.* **165**, 566 (1968).
- [28] S. Sugai, K. Murase, S. Katayama, S. Takaoka, S. Nishi, and H. Kawamura, *Solid State Commun.* **24**, 407 (1977).
- [29] M. Sato, *Phys. Rev. B* **81**, 220504(R) (2010).
- [30] L. Fu and C. L. Kane, *Phys. Rev. B* **76**, 045302 (2007).
- [31] A. Yamakage, K. Yada, M. Sato, and Y. Tanaka, *Phys. Rev. B* **85**, 180509(R) (2012).
- [32] L. Hao and T. K. Lee, *Phys. Rev. B* **83**, 134516 (2011).
- [33] $\text{Pb}_{1-x}\text{Tl}_x\text{Te}$ single crystals were grown by a vapor transport method using high-purity elements of Pb (99.998%), Te (99.999%), and Tl (99.999%). The Tl concentration was measured with ICP-AES and was consistent with the T_c value [34]. For the point-contact experiments, $\text{Pb}_{1-x}\text{Tl}_x\text{Te}$ crystals were cleaved at room temperature in air to obtain a good (001) surface.
- [34] Y. Matsushita, H. Bluhm, T. H. Geballe, I. R. Fisher, *Phys. Rev. Lett.* **94**, 157002 (2005).

Supplemental Material

S1. Soft Point-Contact Spectra on a Conventional Superconductor

To confirm that our soft point-contact technique yields conventional Andreev reflection spectra if applied to a conventional superconductor, we have prepared a soft point contact on an oxidized surface of Sn with the same technique using the same silver paint as the experiment for $\text{Sn}_{1-x}\text{In}_x\text{Te}$. As shown in Fig. S1, the obtained spectra are what is exactly expected for conventional Andreev reflection between a BCS superconductor and a metal. The fitting of the extended Blonder-Tinkham-Klapwijk theory [21] to the data tells us that this junction has an intermediate transparency of $Z = 0.47$.

S2. Origin of the Zero-Bias Conductance Peak

The zero-bias conductance peak (ZBCP) is often observed in point contact experiments on bulk superconductors. Besides the intrinsic Andreev bound state associated with unconventional superconductivity, there are other possible causes of the ZBCP: conventional Andreev reflection [21, 24], heating/critical-current effects [25], reflectionless tunneling [26], and magnetic Kondo scattering [27, 35]. In the following, we show how those other causes of the ZBCP can be dismissed.

The conventional Andreev reflection can give rise to a single ZBCP when the temperature is close to T_c . This is because the two-peak structure characteristic of the conventional Andreev reflection spectra can be blurred into a single peak by thermal fluctuations near T_c . For example, in our data for Sn shown in Fig. S1, one can see a single peak in the data for 3.2 K, which is only 0.5 K below T_c ; as the temperature is lowered, such a single peak splits into two, and the peak separation corresponds to twice the superconducting energy gap, 2Δ . Indeed, in the case of Sn, the peak splits into two at 2.5 K and below, and the peak separation is consistent with 2Δ . On the other hand, because the conductance peak in $\text{Sn}_{1-x}\text{In}_x\text{Te}$ does not split into two even at 0.37 K (which is less than $1/3$ of T_c) and also because pronounced dips rather than peaks are observed at 2Δ , one can safely conclude that the spectra observed in $\text{Sn}_{1-x}\text{In}_x\text{Te}$ is not due to the conventional Andreev reflection.

The heating/critical-current effects cause a spurious ZBCP in samples with a large normal-state resistivity when the contact is in the thermal regime. This is because the increase in the bias voltage causes the local current to exceed the critical current and leads to a voltage-dependent decrease in the differential conductivity. A characteristic feature of the ZBCP of this origin is that the height of the peak changes little with a weak magnetic field, while the width of the ZBCP narrows quickly with increasing H . This is because the conductivity at zero-bias is always measured below the critical current as long as the superconductor is in the zero-resistivity state, whereas the decrease in critical current with magnetic field is directly reflected in the width of the spurious ZBCP. In the magnetic-field

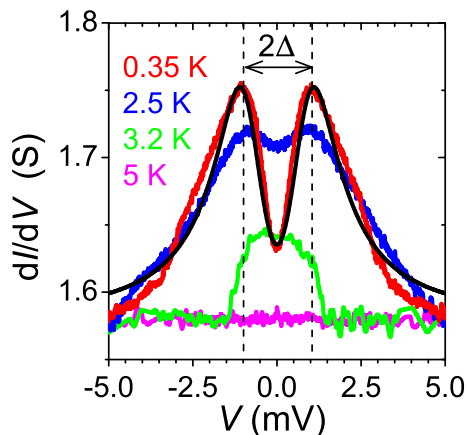


FIG. S1: Andreev reflection spectra measured with the soft point contact technique on a conventional superconductor. Differential conductivity dI/dV vs. bias voltage obtained on an oxidized surface of Sn with our soft point-contact technique. The black solid line is the theoretical fitting to the data at 0.35 K using the extended Blonder-Tinkham-Klapwijk theory, which yields the superconducting gap energy $\Delta = 1.0$ meV, junction transparency $Z = 0.47$, and the broadening parameter $\Gamma = 0.75$ meV.

dependence of the spectra measured on $\text{Sn}_{1-x}\text{In}_x\text{Te}$ [Fig. 2(b) of the main text], the ZBCP is suppressed to about a half of the height at 0 T with a magnetic field of only 0.09 T, but the position of the dips in the spectra does not move inward. Obviously, this speaks against the heating/critical-current origin of the ZBCP. Also, when the critical current is reached in a point contact, it usually causes a sharp, spike-like dip in the dI/dV data [21, 25], which reflects a rapid increase in voltage with a small change in current. The absence of such spikes in our data corroborates our conclusion that the heating/critical-current effect is not relevant to the observed ZBCP.

In the case of the reflectionless tunneling [26], the conductance peak is caused by the coherent backscattering of electrons in the normal metal. Such a coherent backscattering is suppressed with a magnetic field because it breaks time-reversal symmetry, and the characteristic magnetic field for the suppression is estimated with the condition that the magnetic flux threading a coherent path of the electrons (which is set either by the size of the normal metal or by the electron dephasing length L_ϕ) is equal to the flux quantum $\Phi_0 (= h/2e)$. The footprint of our point contact has the diameter of $\sim 20 \mu\text{m}$, which is larger than the dephasing length L_ϕ of $\sim 1 \mu\text{m}$ in Ag below 1 K [36]. This means that L_ϕ governs the reflectionless tunneling [26] which would be suppressed with only ~ 0.7 mT. Given that the ZBCP is still visible in 0.2 T in the present case, the reflectionless tunneling is not likely to be its origin. Also, the reflectionless tunneling is a weak effect and can never cause a doubling of the zero-bias conductance.

Another well-known origin of the ZBCP is the magnetic Kondo scattering [27, 35]. One should remember that the ZBCP of this origin is expected even in the normal state, and, hence, the fact that the ZBCP in $\text{Sn}_{1-x}\text{In}_x\text{Te}$ shows up only in the superconducting state already speaks against this possibility. Furthermore, the g factor of SnTe is expected to be more than 20 for the valence band [37], which suggests that the Zeeman splitting for $S = 1/2$ in 0.1 T would be larger than 0.1 meV. This should be observable in our data if the magnetic scattering is relevant. Hence, the absence of peak splitting in 0.1 T gives further evidence against the relevance of the magnetic Kondo scattering in the ZBCP.

* Electronic address: liangfu@mit.edu

† Electronic address: y.ando@sanken.osaka-u.ac.jp

[13] S. Sasaki, M. Kriener, K. Segawa, K. Yada, Y. Tanaka, M. Sato, and Y. Ando, Phys. Rev. Lett. **107**, 217001 (2011).

[21] D. Daghero and R. S. Gonnelli, Supercond. Sci. Technol. **23**, 043001 (2010).

[24] G. E. Blonder, M. Tinkham, and T. M. Klapwijk, Phys. Rev. B **25**, 4515 (1982).

[25] G. Sheet, S. Mukhopadhyay, and P. Raychaudhuri, Phys. Rev. B **69**, 134507 (2004).

[26] C. W. J. Beenakker, Phys. Rev. B **46**, 12841(R) (1992).

[27] L. Y. L. Shen and J. M. Rowell, Phys. Rev. **165**, 566 (1968).

[35] J. Appelbaum, Phys. Rev. Lett. **17**, 91 (1966).

[36] P. McConville and N. O. Birge, Phys. Rev. B **47**, 16667(R) (1993).

[37] R. L. Bernick and L. Kleinman, Solid State Commun. **8**, 569 (1970).